Chemical Physics Letters 458 (2008) 101–107

Contents lists available at ScienceDirect

Chemical Physics Letters

journal homepage: www.elsevier.com/locate/cplett

Local atomic structure and chemical bonding in liquid Te: An *ab initio* molecular-dynamics simulation

G. Zhao [a,*], C.S. Liu [b], Z.G. Zhu [b]

[a] Department of Physics and Electronic Engineering, Ludong University, Hongqi Road, No. 186, Yantai 264025, PR China
[b] Key Laboratory of Materials Physics, Institute of Solid State Physics, Chinese Academy of Sciences, P.O. Box 1129, Hefei 230031, PR China

ARTICLE INFO

Article history:
Received 17 March 2008
In final form 28 April 2008
Available online 4 May 2008

ABSTRACT

Local atomic structure and chemical bonding in liquid Te were investigated by *ab initio* molecular-dynamics simulations and inherent structure formalism. Our results first present two types of Peierls distorted local structures in liquid Te. Accompanying the shoaling of the dip at E_F in DOS from 573 to 1073 K, the interchain distances are shortened and the tendency of short-long alternation of bonds within the chains of atoms becomes stronger. Our results suggest stronger interchain correlation and short-long alternation of bonds within chains may both play important roles on the metallic nature of liquid Te.

1. Introduction

At normal temperature and pressure, crystalline tellurium (Te) is semiconducting trigonal phase, with helical chains of atoms running along the axes of the hexagonal cell and a coordination number of 2 [1]. Upon melting at about 723 K, this chain structure is disrupted and liquid Te shows a metallic-like behavior despite of the covalently bound atoms and a coordination number of 2.5 [2,3]. Moreover, many thermophysical properties of liquid Te show striking anomalies ranging from the equilibrium liquid above melting point down to the supercooled state [4,5]. For example, liquid Te exhibits a minimum volume at about 733 K, with decreasing temperature from melting point (723 K) to 573 K, supercooled liquid Te undergoes an abnormal volume expansion, which is accompanied by a very sharp extreme at about 623 K in thermal expansion coefficient, adiabatic compressibility, and constant pressure heat capacity, respectively. These anomalies indicate the occurrence of rapid structural change in liquid Te from normal- to supercooled-state. But the driving mechanism for structural change is still open. For these two reasons, liquid Te remains an object of interest for many researchers in the past several decades.

Generally, there are close relations between physical properties and liquid structures. Liquid structure is usually understood with reference to its crystal structure. The trigonal structure of crystalline Te is usually discussed in terms of a Peierls distortion of simple cubic lattice [6]. For Te, the p bands is two-thirds filled, the lattice is unstable against a Peierls distortion dividing the six nearest-neighbor bonds into two short intrachain bonds (0.284 nm) and four long interchain bonds (0.349 nm) [1,7]. Although the concept of Peierls distortion was established in the context of low dimensional and periodic structures, recently it has been generalized for aperiodic systems using direct space method [7].

During the past three decades, to explain the metallic-like behavior and the anomaly of thermophysical properties, there are many data about the atomic structure and chemical bonding in liquid Te. Most of the results from X-ray or neutron scattering experiments showed that the coordination number in liquid Te is about 3 at higher temperature and 2.5 at melting point, which is larger than that in crystalline Te [3], indicating it is not a pure chain structure in liquid Te. Indeed, a molecular-dynamics simulation of the structure of liquid Te based on effective interatomic forces derived from pseudopotential theory described the structure in terms of 'entangled broken chains' [8]. Misawa also suggested that the experimental structure factors and pair-correlation functions can be explained using a short-chain model [9]. Additionally, Menelle et al. [10] suggested a splitting of the first coordination shell into two different kinds of atoms: the two covalently bound atoms corresponding to the crystal structure and a third atom at a slightly larger distance. According to the analysis from the EXAFS data of Tsuzuki et al. [11,12], the first coordination shell can be thought of as the superposition of two Gaussians centered at a short and long bond length (0.282 and 0.301 nm at 753 K) inside the first peak of $g(r)$, and there is a strong interchain correlation between the chains at melting point. As decreasing temperature from melting point, the number of long bonds is reduced and the local structure changes substantially accompanied by the reduction of interchain correlation. Moreover, they argued that the long bonds and the strong interchain correlation are associated with the metallic nature of liquid Te. By tight-bonding Monte Carlo simulation, Bichara et al. [13] showed that on melting, the chain structure of crystalline Te is preserved and a short-long alternation (0.280 nm and 0.290 nm) of bonds takes place within the chains. The local environment of each atom changes from two short and four long

* Corresponding author.
E-mail address: gzhao19800209@126.com (G. Zhao).

0009-2614/$ - see front matter © 2008 Elsevier B.V. All rights reserved.
doi:10.1016/j.cplett.2008.04.113

neighbor distances to two short, one medium, and three long neighbor distances. Analysing the EXAFS data for supercooled liquid Te by adopting a 'model-independent' method, Kawakita et al. [14] found that the short chains in liquid Te with metallic nature are composed of short (0.280 nm) and long (0.295 nm) covalent bonds. At the same time, there are some different points of view. For example, the results from Molina and Lomba [15] suggested a continuous distribution of bond lengths from 0.25 to 0.33 nm. They demonstrated that, the opinion about short and long bond length inside the first peak of $g(r)$ may be a rather naive view of the nearest neighbor structure, and it might actually be the case that the continuous distribution, even if it can be represented by the superposition of two Gaussians, is the only true physical representation of the microscopic structure. They also pointed out that a more clear picture about whether there exist a short bond and a long one inside the first peak of $g(r)$, i.e. a short-long alternation of bonds within the chains, can be obtained if inherent structure is derived. The 'inherent structure' formalism [16,17], introduced by Stillinger and Weber, is an insightful approach to study the local structure of liquid and amorphous states. It is a way to partition the configuration space for the vibrations of a n-body system into various regions. Within each region, there is one local minimum of the potential-energy surface that can be reached by a minimization algorithm, and the structure at local minimum is the inherent structure of the corresponding region.

In this work, to gain the nature of metallic behavior of liquid Te and analyse the possible reason for the anomaly of thermophysical properties, we have investigated the structural and chemical bonding in liquid Te from 1073 to 573 K, by *ab initio* molecular-dynamics simulations and inherent structure formalism. The paper is organized as follows: in Section 2, we describe the method of simulations; the results and corresponding discussions are reported in Section 3; a conclusion is given in Section 4.

2. Computational methods

Our simulations were performed within the framework of density function theory (DFT) [18]. We used Vienna *ab initio* simulation package (VASP) [19,20], and employed projector augmented-wave (PAW) potential [21,22], with generalized gradient approximation (GGA) formulated by Perdew and Wang (PW91) to the exchange-correlation energy [23,24]. The system (80 Te atoms) was put in a simple cubic box with periodical boundary conditions. The Γ point was used to sample the Brillouin zone of the supercell. The electronic wave functions were expanded in plane wave basis set, with an energy cutoff of 175 eV. Our canonical ensemble simulations were performed at 1073, 843, 673, 623, and 573 K with a Nosé thermostat for temperature control [25]. The experimental density ρ_0, listed in Table 1, was used [4,5]. The Verlet algorithm was used to integrate Newton's equations of motion and the time step of ion motion was 4 fs. The Kohn-Sham energy functional was minimized by preconditioned conjugate-gradient method. An improved Pulay-mixing [26] is used to achieve self-consistency of charge-density and potential.

The initial atomic configuration adopted was a random distribution of 80 atoms on the grid, which was constructed by dividing the supercell into $5 \times 5 \times 5$ square segments. Then, the system was heated up to 1073 K by rescaling the ionic velocities. After a run of 20 ps at this temperature, the system arrived at an equilibrium liquid state. Another run of 16 ps was performed to obtain 4000 configurations (called general structure configurations) for analyzing the physical quantities of interest. Then gradually reducing temperature to 843 K, the physical quantities were also obtained by averaging over 16 ps after the equilibration taking 8 ps. For other temperatures, we only repeated this procedure and changed the final temperature into 673, 623, and 573 K, respectively. At 1073 and 573 K, we obtained 20 configurations during the run of 16 ps and relaxed them to their closest local minima (corresponding configurations are called inherent structure configurations) by a conjugate gradient energy minimization algorithm [16,17], and then analyzed the inherent structure by averaging the 20 inherent structure configurations.

Table 1
Main features of general $g(r)$

Temp. (K)	ρ_0 (at/Å^3)	R_1 (Å)	R_{min} (Å)	R_2 (Å)	r_{max} (Å)	CN
573	0.0262	2.89 (2.87)	3.70 (3.75)	4.33 (4.31)	2.95	2.25
623	0.0266	2.92	3.82	4.36	2.98	2.51
673	0.0271	2.95	3.73	4.30	3.04	3.04
843	0.0270	2.95	3.76	4.30	3.07	3.35
1073	0.0262	2.95 (2.87)	3.88 (3.62)	4.30 (4.31)	3.07	3.41

ρ_0: density used; R_1 and R_2: respectively, first- and second-peak position; R_{min}: first minimum position; r_{max}: first-peak position in RDF; CN: coordination number. Main features of inherent $g(r)$ are given in parentheses.

3. Results and discussion

In a molecular dynamics simulation of liquid state, structure factor $S(Q)$ serves as a connection with experimental results. $S(Q)$ can be obtained from atomic coordinates,

$$S(Q) = \frac{1}{N}\left\langle \sum_i \sum_{j\neq i} \exp(-i\vec{Q}\cdot\vec{r}_{ij}) \right\rangle - N\delta_{Q,0}, \quad (1)$$

where N is total number of atoms, r_{ij} is interatomic distance between atoms i and j. $S(Q)$ can also be obtained by Fourier transformation of pair-correlation function $g(r)$. Our calculated results by the two methods and experimental data are both shown in Fig. 1a. It can be found that the calculated structure factors by the two methods are in good agreement with each other. As can also be seen, at 1073 K, the calculated $S(Q)$ is in good agreement with experimental result [9], although there are discernible shifts especially from 30 to 60 nm^{-1}. At 573 K, compared to experimental data at 603 K [3,10], although the shifts become more obvious, the overall agreement between them is acceptable. It should be noticed that, compared to experimental results [3,10], our results reproduce the evolution of $S(Q)$: with increasing temperature, the height of the second peak decreases monotonously from 573 to 1073 K, however, that of the first peak shows a non-monotonous temperature-dependence. Fig. 1b plots the first-peak height of $S(Q)$ as a function of temperature. It can be seen that, with increasing temperature, the first-peak height increases from 573 to 673 K and decreases from 843 to 1073 K, leading to an obvious extreme at around 723 K. This is in good agreement with the anomaly of thermophysical properties observed in experiments [4]. So we believe that the discrepancy in $S(Q)$ between our results and experimental data does not hamper our analysis of the structural changes in liquid Te.

The pair-correlation function $g(r)$ can be calculated according to Eq. (2),

$$g(r) = \frac{1}{\rho_0 N}\left\langle \sum_i \sum_{j\neq i} \delta(\vec{r}-\vec{r}_{ij}) \right\rangle. \quad (2)$$

The calculated results are shown in Fig. 2a and the main features of $g(r)$ are summarized in Table 1. It should be noticed that the first peak is asymmetry and there is a shallow trough between the first and the second peaks, indicating a nonsimple local structure in liquid Te. With increasing temperature, the heights of the peaks decrease, and the trough becomes more and more shallow, almost

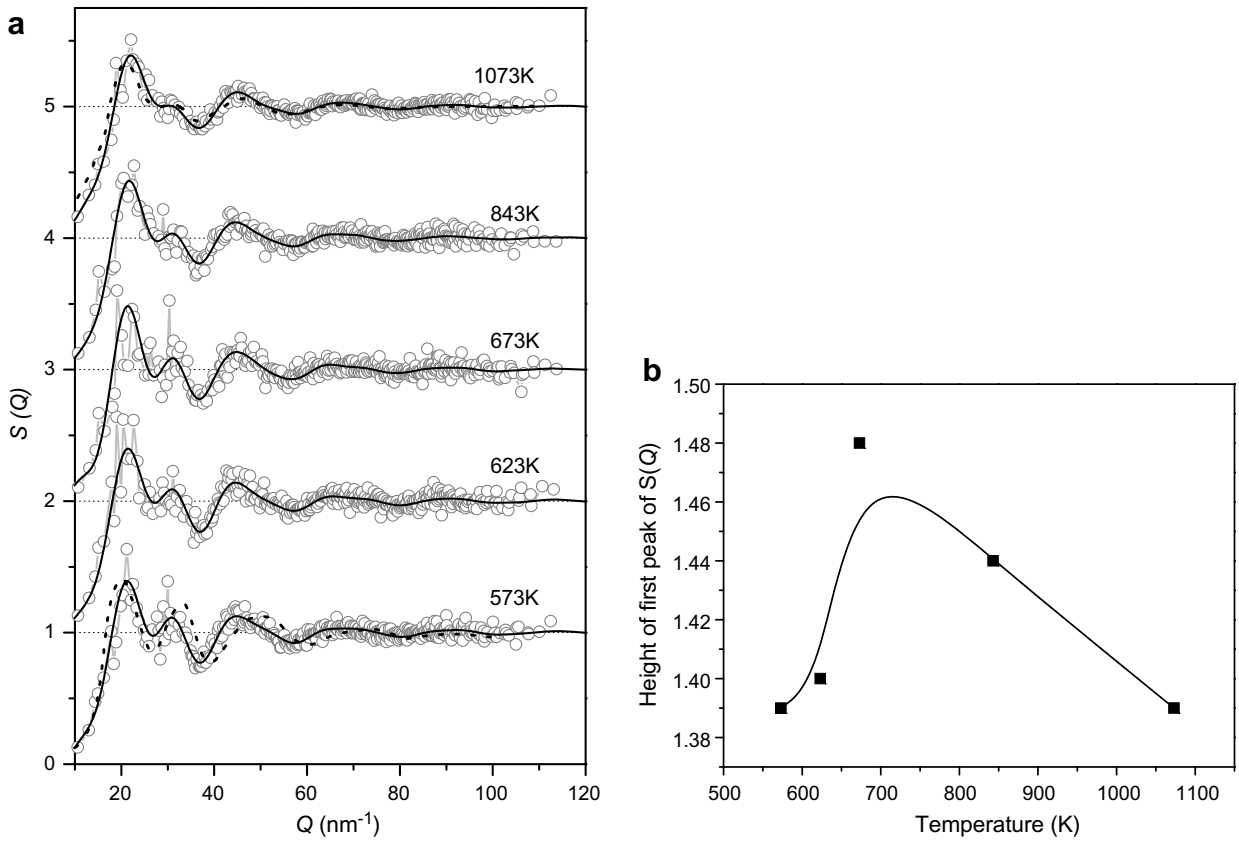

Fig. 1. (a) Structure factors of liquid Te calculated by Fourier transform (solid line) and direct calculation (grey line and circle), compared with experimental data (dash line) at 1073 K from Ref. [9] and 603 K from Ref. [10]. (b) Temperature-dependent height of the first peak in $S(Q)$ of simulated liquid Te.

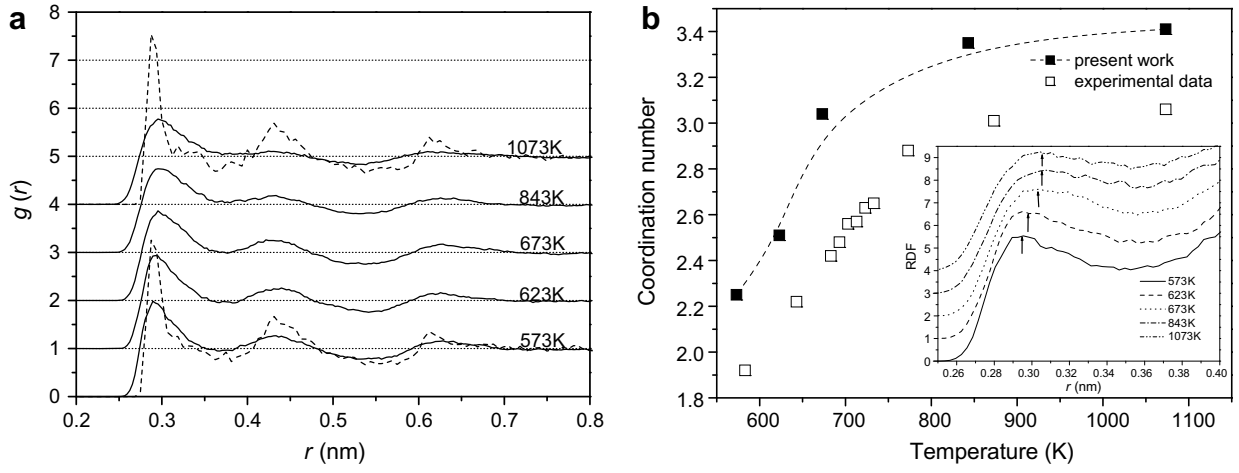

Fig. 2. (a) Calculated pair-correlation functions of liquid Te from general structures (solid line) and inherent structures (dash line). (b) Calculated average coordination number compared with experimental data from Refs. [3,12]. The inset displays RDF and the arrow indicates the position of the first peak.

disappears at 1073 K. The evolution of these features is in good agreement with experimental results [3,10]. In order to verify whether a short-long alternation of bonds (about 0.280 and 0.295 nm) takes place within the chains of atoms in liquid Te, we also calculated $g(r)$ from inherent structures at 573 and 1073 K. The calculated results are also shown in Fig. 2a. We can find that the first peak in $g(r)$ from inherent structures, is more sharp than that in $g(r)$ from general structures. Although the splitting of the first peak does not occur, an obvious shoulder appears in the right-hand side of the first peak about 0.340 nm. The positions of the first peak and the shoulder are very close to the two characteristic bond lengths of Peierls distortion in trigonal Te (0.284 nm and 0.349 nm [7]), indicating that Peierls-type distorted local structure similar to that in crystalline Te can be still preserved at 1073 and 573 K. Through the analysis on angular limited bond–bond correlation functions, we find that this is indeed the case, as will be seen in the following parts of this section. Given $g(r)$, the average coordination number (CN) can be estimated as in Ref. [27],

$$N = 2\int_0^{r_{max}} 4\pi r^2 \rho_0 g(r)\mathrm{d}r, \quad (3)$$

where r_{max} is the position of the first peak in radial distribution function (*RDF*) $4\pi r^2\rho_0 g(r)$. *RDF*, r_{max}, and CN, are all shown in Fig. 2b. One can find that, r_{max} increases gradually from 573 to 673 K; however, it hardly depends of temperature from 843 to 1073 K. Correspondingly, CN increases steadily from 573 to 673 K, which is in contrast to the behavior of a classical isotropic fluid. This suggests that, with decreasing temperature from 673 to 573 K, the volume expands and hence a negative thermal-expansion coefficient is observed. However, from 843 to 1073 K, CN seems almost unchanged. The experimental data [3,12] are also shown in Fig. 2b. An overestimation of CN can be found. As demonstrated in Ref. [28], it is due to GGA used on the exchange–correlation functional, leading to the right shift and the overestimation of the width of the first neighbor peak. However, the evolution of CN with temperature is in good accordance with experimental results.

To obtain more microscopic atomic structure information, we have also calculated the bond-angle distribution function $g_3(\theta)$—one type of three body distribution functions. The angle noted in $g_3(\theta)$ is formed by two vectors drawn from a reference atom to any other two atoms within a sphere of cutoff radius r_{cutoff}. Fig. 3a gives the calculated $g_3(\theta)$ from general structures. When $r_{cutoff} = 0.360$ nm, including the first peak and the shoulder in its right side in $g(r)$ from inherent structures, $g_3(\theta)$ shows three peaks. The first peak, located at around 60°, is related to close-packed structure of atoms. Its height increases with increasing temperature, indicating close-packed structure of atoms becomes more close-packed. The second peak is located at $\theta \sim 90°$, slightly less than that in trigonal Te ($\theta \sim 103°$ [1,7]). Its height increases with decreasing temperature. Additionally, the third peak is located at around $\theta \sim 155°$. It shifts left with increasing temperature but its height is almost unchanged. When $r_{cutoff} = 0.300$ nm, not including the shoulder, the 60° peak almost disappears and the 155° peak becomes more lower. However, the second peak becomes more higher and moves to about 96°. We have also calculated $g_3(\theta)$ from inherent structures at 1073 and 573 K. The results are shown in Fig. 3b. When $r_{cutoff} = 0.360$ nm, compared to $g_3(\theta)$ from general structures, the 60° peak is more lower, while the second and the third peaks become more obvious and the height of them is more higher. Moreover, the third peak appears at about 167°. The second and the third peaks seem to indicate a Peierls-like distorted local structure similar to that in crystalline Te is still preserved at 1073 and 573 K. This is consistent with that found in $g(r)$ from inherent structures (as shown in Fig. 2a). When $r_{cutoff} = 0.300$ nm, the first and the third peaks disappear completely, indicating that at least one of the two bonds which form the 167° angle is included in the shoulder. The second peak moves to 100°, very close to that in crystalline Te ($\theta \sim 103°$, formed by two adjacent bonds in the chain of atoms), implying the chain structure of the crystalline Te is still remained in liquid Te. This is consistent with the results of simulations by Bichara et al. [13] and experimental observation by Kawakita and co-workers [14].

To obtain direct evidences of a Peierls-type distorted local structure and a short-long alternation of bonds within the chains, we have also calculated the angular limited bond-bond correlation function from inherent structures as introduced in Ref. [29]. This function $P(r_1, r_2)$ is defined as the probability of finding an atom

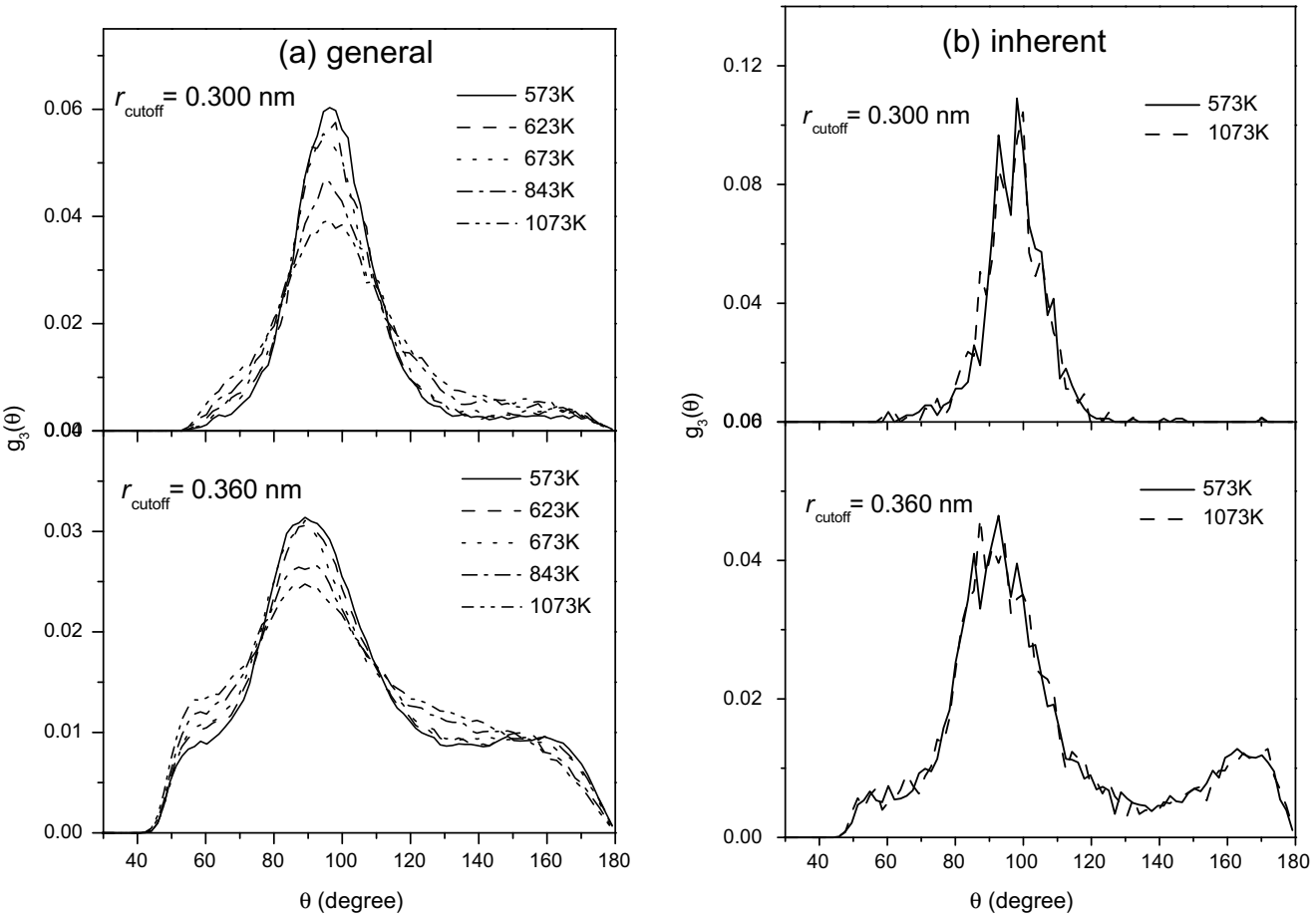

Fig. 3. Calculated bond-angle distribution functions from (a) general structures and (b) inherent structures.

C at a distance r_2 from an atom B, which is at a distance r_1 from the reference atom A. A constraint is placed on the position of atom C. Namely, the angle θ formed by vectors $\vec{BA}$ and $\vec{BC}$ is constrained in a small range. Here, in order to investigate the correlation of two bonds which form the angle about 167° (*i.e.*, the third peak in $g_3(\theta)$ from inherent structures), θ is chosen between 160° and 170°. The result is shown in Fig. 4a. At 1073 K, the maxima of $P(r_1, r_2)$ are mainly centered at four regions (0.285, 0.340 nm), (0.340, 0.285 nm) and (0.290, 0.320 nm), (0.320, 0.290 nm). This indicates that a short bond of length r_1 (0.285 nm or 0.290 nm) is most probably followed by a longer bond of length r_2 (0.340 nm or 0.320 nm), and vice versa. The values that $r_1 = 0.285$ nm and $r_2 = 0.340$ nm are very close to the characteristic bond length of Peierls distortion in trigonal Te (0.284 nm and 0.349 nm [1,7]). This indicates that Peierls-type distorted local structure similar to that in crystalline Te is preserved at 1073 K. The values that $r_1 = 0.290$ nm and $r_2 = 0.320$ nm indicate the occurrence of two new characteristic bonds in liquid Te. The bond length 0.290 nm is inside the first peak of $g(r)$, and the bonding is clearly covalent. The occurrence of the bond length 0.320 nm is in accordance with observations by different researchers [13,10,12], although 0.320 nm is slightly larger than experimental and theoretical results 0.310 nm. Moreover, from our results, it can be found that the two bonds $r_1 = 0.290$ nm and $r_2 = 0.320$ nm also formed a Peierls-type distorted local structure, although the bond lengths are different from those in crystalline Te. The existence of the characteristic bonds with bond length $r_2 = 0.340$ nm and $r_2 = 0.320$ nm also shows that an interchain correlation exists between the chains of atoms. But it should be noticed that the two bonds, especially $r_2 = 0.320$ nm, are both shorter than that in crystalline Te 0.349 nm, indicating that interchain correlation at 1073 K is stronger than that in crystalline Te. The characteristic bond lengths 0.285 nm and 0.290 nm are both inside the first peak of $g(r)$, suggesting a short-long alternation of bonds within the chains of atoms. It can also be concluded that, the reason that the splitting of the first peak in $g(r)$ from inherent structures does not occur (as shown in Fig. 2a), may be due to the lengths of the two bonds are very close. Compared to the results at 1073 K, one can find that, at 573 K, the two shorter bonds 0.285 and 0.290 nm are unchanged, but the two longer bonds become from 0.320 and 0.340 nm at 1073 K to 0.330 and 0.345 nm at 573 K, respectively. This indicates that interchain correlation reduces when decreasing temperature from 1073 to 573 K. Obviously, the Peierls-type distorted local structures at 573 K correspond to larger atomic volume than

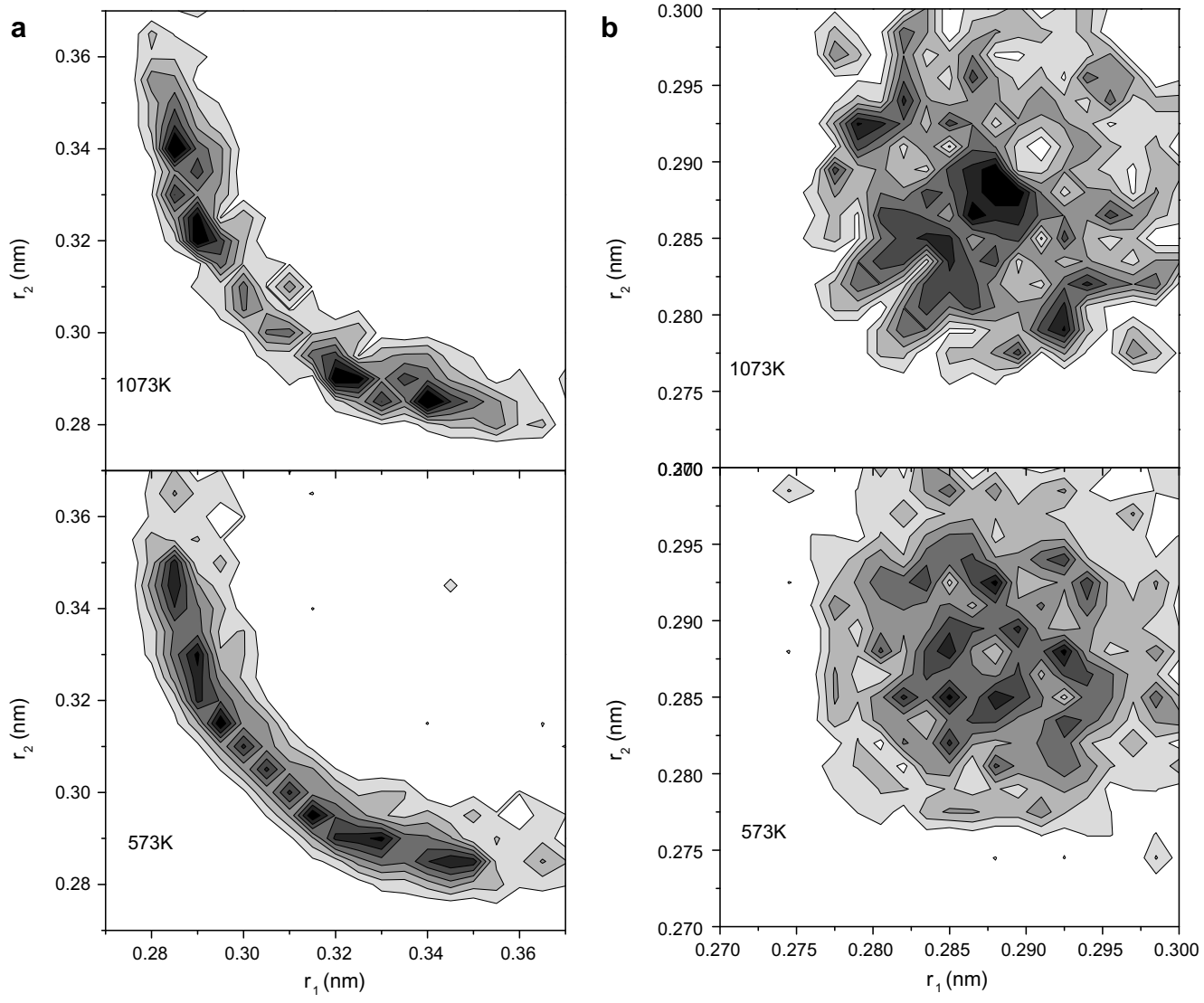

Fig. 4. Calculated angular limited bond-bond correlation function (a) $\theta \sim 167^\circ$ and (b) $\theta \sim 100^\circ$ at 573 and 1073 K.

that at 1073 K. It can be expected that, with decreasing temperature, the lengths of two short intrachain bonds are unchanged, but that of two long interchain bonds become longer and longer, so that the Peierls-type distorted local structures occupy larger and larger volume, resulting in the experimentally observed abnormal volume expansion from 723 to 573 K. So our results suggest that the change of Peierls-type distorted local structure with temperature may be responsible for the anomalies of thermophysical properties of liquid Te. To further clarify the short-long alternation of bonds within the chains of atoms, the correlation of two bonds which form the angle about 100° (*i.e.*, the second peak in $g_3(\theta)$ from inherent structures) has also been calculated. Here, θ is chosen between 90° and 110°. The results are shown in Fig. 4b. It can be seen that, at 1073 K, the maxima of $P(r_1, r_2)$ are mainly centered at three regions (0.280, 0.292 nm), (0.292, 0.280 nm) and (0.288, 0.288 nm). The values that $r_1 = 0.280$ nm and $r_2 = 0.292$ nm indicate that there is a stronger tendency to alternate long and short bonds in the chains of atoms. This is in agreement with the recent experimental results (0.282 and 0.299 nm) [11,12] and theoretical results (0.280 and 0.290 nm) [13]. However, at 573 K, several very small regions of short-long and long-short bonds correlation are observed, suggesting the tendency of short-long alternation of bonds is no more stronger.

The microscopic atomic structure is correlated with electronic structure. Here we also studied the electronic density of state (DOS) and local density of states (LDOS), i.e., the DOS is decomposed into angular-momentum-resolved contributions. The calculated results are represented in Fig. 5. We can see that the major contribution to DOS at the Fermi level E_F is mainly due to Te p orbital. Besides the feature of bond-angle distribution function mentioned above, this feature of DOS is indeed another condition that has to be fulfilled to allow a Peierls distortion of the local atomic environment as explained in Ref. [7]. It can also be found that there is no gap in DOS at E_F, demonstrating metallic-like behavior, but a small 'dip' still exists, which mainly results from Te p orbital. But it should also be noticed that the dip at 1073 K is more shallow than that at 573 K.

Based on our present results, we now turn to the metallic nature of liquid Te. As demonstrated by Bichara et al. [13], when one of the interchain distances is shortened, a resonance effect arises between two neighboring lone pair orbitals, leading to the broadening of lone pair band. This is responsible for the SC-M transition that takes place upon melting. Here, we assurely find that, accompanying the shoaling of the dip at E_F from 573 to 1073 K, the interchain distances are shortened. Therefore, according to above explanation, our results seems to imply that the stronger interchain correlation may be one of the reasons associated with the metallic nature of liquid Te. Recently, in the explanation of SC-M transition that occurs with density decrease in liquid Se at high temperature and pressure, Yonezawa et al. [30,31] attribute the leading role in the SC-M transition to the presence of short and long bonds. When the volume is expanded, some of the bonds are more stretched than others because of the fluctuations due to thermal effects. The presence of these long bonds lower the antibonding p band, inducing an overlap with the nonbonding p states. In this explanation, the existence of short and long intrachain covalent bonds is the crucial factor in the formation of conduction band. In our work, accompanying the shoaling of the dip at E_F, the short-long alternation of bonds within the chains of atoms becomes more stronger from 573 to 1073 K. So our results seem to also support this proposed SC-M transition mechanism, i.e., the alternation of long and short bonds in the atomic chains may be another reason associated with the metallic nature of liquid Te, besides the stronger interchain correlation mentioned above.

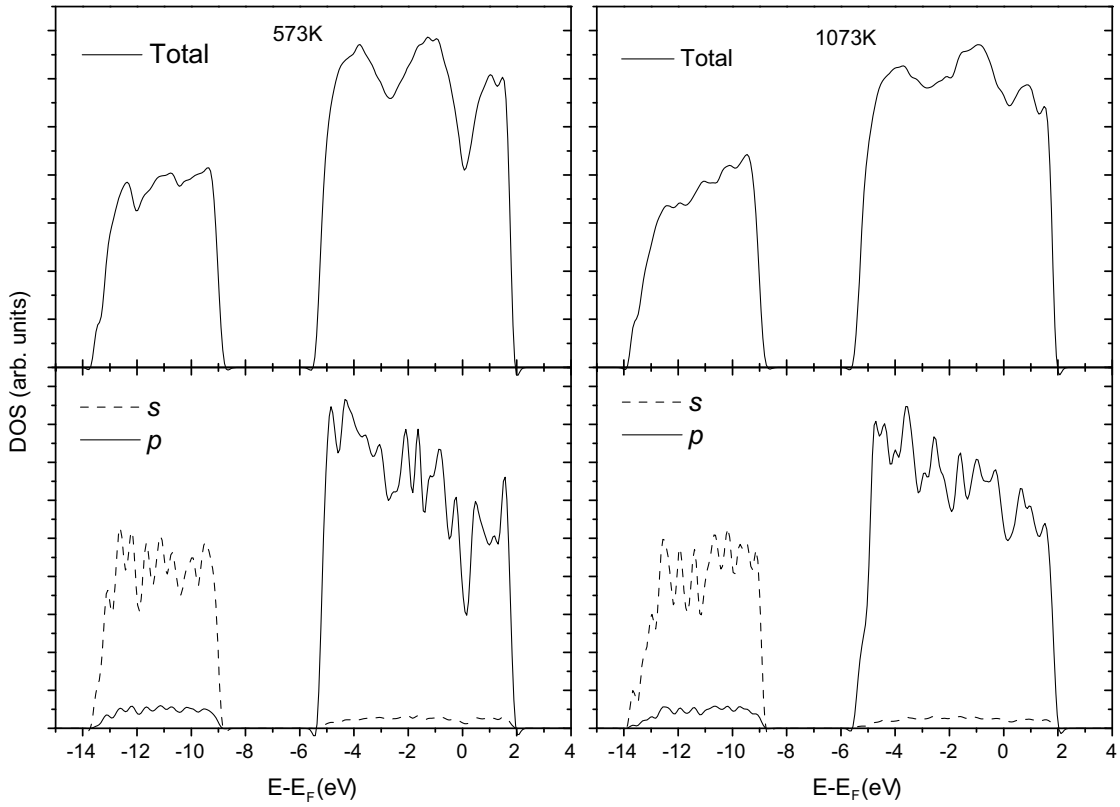

Fig. 5. Total and local electronic density of states of liquid Te at 573 and 1073 K.

4. Conclusions

In conclusion, the local atomic structure and chemical bonding in liquid Te from 573 to 1073 K were investigated by *ab initio* molecular-dynamics simulations and inherent structure formalism. Our results reproduce the experimental observation and first show that there are two types of Peierls distorted local atomic structures in liquid Te: one is similar to that in crystalline Te, but the other is different. Accompanying the shoaling of the dip at E_F in DOS from 573 to 1073 K, the interchain distances are shortened and the short-long alternation of the bonds within the atomic chains becomes more and more stronger. Our results seem to suggest that, the stronger interchain correlation and the alternation of long and short bonds in the atomic chains may both play important roles on the metallic nature of liquid Te. Our results also suggest that the anomaly of thermophysical properties of liquid Te may also be related to the variation of Peierls-type distorted local structure with temperature.

References

[1] W.B. Pearson, The Physics and Chemistry of Metals and Alloys, Wiley, New York, 1972.
[2] J.C. Perron, Adv. Phys. 16 (1967) 657.
[3] A. Menelle, R. Bellisent, A.M. Flank, Europhys. Lett. 4 (1987) 705, and references therein.
[4] Y. Tsuchiya, J. Phys. Soc. Jpn. 60 (1991) 227.
[5] Y. Tsuchiya, J. Phys.: Condens. Matter 3 (1991) 3163.
[6] G. Kresse, J. Furthmüller, J. Hafner, Phys. Rev. B 50 (1994) 13181, and references therein.
[7] J.P. Gaspard, A. Pellegatti, F. Marinelli, C. Bichara, Philos. Mag. B 77 (1998) 727, and references therein.
[8] J. Hafner, J. Phys.: Condens. Matter 2 (1990) 1271, and references therein.
[9] M. Misawa, J. Phys.: Condens. Matter 4 (1992) 9491.
[10] A. Menelle, R. Bellisent, A.M. Flank, Physica B 156&157 (1989) 174.
[11] T. Tsuzuki et al., J. Non-Cryst. Solids 156–158 (1993) 695.
[12] T. Tsuzuki, M. Yao, H. Endo, J. Phys. Soc. Jpn. 64 (1995) 485.
[13] C. Bichara, J.Y. Raty, J.P. Gaspard, Phys. Rev. B 53 (1996) 206.
[14] Y. Kawakita, M. Yao, H. Endo, J. Non-Cryst. Solids 250-252 (1999) 447.
[15] D. Molina, E. Lomba, Phys. Rev. B 67 (2003) 094208, and references therein.
[16] F.H. Stillinger, Science 267 (1995) 1935.
[17] S. Sastry, P.G. Debenedetti, F.H. Stillinger, Nature 393 (1998) 554 (London).
[18] W. Kohn, L.J. Sham, Phys. Rev. 140 (1965) A1133.
[19] G. Kresse, J. Furthmüller, Phys. Rev. B 54 (1996) 11169.
[20] G. Kresse, J. Furthmüller, Comput. Mater. Sci. 6 (1996) 15.
[21] P.E. Blöchl, Phys. Rev. B 50 (1994) 17953.
[22] G. Kresse, D. Joubert, Phys. Rev. B 59 (1999) 1758.
[23] Y. Wang, J.P. Perdew, Phys. Rev. B 44 (1991) 13298.
[24] J.P. Perdew, J.A. Chevary, S.H. Vosko, K.A. Jackson, M.R. Pederson, D.J. Singh, C. Fiolhais, Phys. Rev. B 46 (1992) 6671.
[25] S. Nosé, J. Chem. Phys. 81 (1984) 511.
[26] P. Pulay, Chem. Phys. Lett. 73 (1980) 393.
[27] J. Mizuki, K. Kakimoto, M. Misawa, T. Fukunaga, N. Watanabe, J. Phys.: Condens. Matter 5 (1993) 3391.
[28] R. Stadler, M.J. Gillan, J. Phys.: Condens. Matter 12 (2000) 6053.
[29] C. Bichara, A. Pellegatti, J.P. Gaspard, Phys. Rev. B 47 (1993) 5002.
[30] F. Yonezawa, H. Ohtani, T. Yamaguchi, J. Phys.: Condens. Matter 10 (1998) 11419.
[31] F. Yonezawa, H. Ohtani, T. Yamaguchi, J. Non-Cryst. Solids 250–252 (1999) 510.